# A posteriori impact identification

L. JANKOWSKI and M. WIKLO

*Proc. of the 3rd European Workshop on Structural Health Monitoring,*
*5-7 July, Granada, Spain, 2006. pp. 675-682.*

## ABSTRACT

The paper presents a methodology for an a posteriori identification of impact characteristics and its development. The motivation of the paper is the need for a general post-impact analysis technique for efficient identification of the cause and the scenario of a collision or a collapse. The proposed approach can be applied in a black box type systems for an accurate post-accident diagnosis [1, 2].

The methodology is based on analysis of local accelerations/strains developing during the impact, includes both elastic and elasto-plastic structural behaviour and can be reformulated to cover other general non-linear effects. It is fully applicable to all impact-exposed engineering structures, provided a dedicated sensors system is distributed in the structure to measure and store local response.

The identification itself is treated as an inverse problem and thanks to the Virtual Distortion Method (VDM) [3] can be formulated analytically as a complex optimisation problem: find the impact scenario that minimises the mean-square distance between simulated and measured dynamic responses in sensor locations. The significant computational effort of the problem is drastically reduced by the VDM approach, which makes possible an analytical sensitivity analysis and does not require actualisation of the global stiffness matrix in the plastic yield phase. Compared to other researches [4, 5, 6] this formulation comprises simultaneous multiple impact and moving loads cases. Additionally, the paper proposes robust hybrid algorithms combining heuristic and gradient-based optimisation techniques, illustrated in a numerical example. A similar approach has been used in parallel research on structural adaptation to impact loads [7].

## VDM: STRUCTURAL DYNAMIC RESPONSE

The methodology is based on the Virtual Distortion Method (VDM), and is thus restricted to small deformation case. Dynamics of an elasto-plastic structure is described in terms of so-called dynamic (or impulse) influence matrices, which store structural response to local impulse excitations of Dirac type and can be either

Smart Technology Centre, Institute for Fundamental Technological Research,
Polish Academy of Sciences, ul. Swietokrzyska 21, 00-049 Warszawa, Poland,
E-mail: (ljank | mwiklo)@ippt.gov.pl

generated from a numerical model or measured experimentally, the latter being potentially more practical in case of real-world complex structures. The measurands can include local displacements and strains, which are easily measured with piezo transducers. Accelerations are also feasible, provided the response is discretised.

The load identification procedure relies on the provided matrices only, and as they retain full information about the modelled structure (including the boundary conditions) there is no need for additional modelling. Therefore, although this paper deals with modelled trusses, the concept is applicable to all types of structures.

**Displacements and strains**

The approach discretises the considered time interval into a finite number of time steps, which are denoted further on by $t$ and $\tau$. The displacement $u_i(t)$ in the $i$-th degree of freedom (DOF) of the analysed structure is a linear combination of the responses to all previous loading forces $p_n(\tau)$ (occurring in DOFs $n \in \boldsymbol{L}$) and plastic distortions (occurring in plastified elements $\xi \in \boldsymbol{\Xi}$), and can be expressed as follows:

$$u_i(t) = \sum_{\tau=0}^{t} \sum_{n \in \boldsymbol{L}} D^P_{in}(t-\tau)\, p_n(\tau) + \sum_{\tau=0}^{t} \sum_{\xi \in \boldsymbol{\Xi}} D^{\varepsilon}_{i\xi}(t-\tau)\, \beta_{\xi}(\tau). \tag{1}$$

The Latin indices in Eq. (1) and thorough the paper denote degrees of freedom (DOFs), while the Greek indices are reserved for truss elements. The matrices $\boldsymbol{D^P}$ and $\boldsymbol{D^{\varepsilon}}$ are the above-mentioned dynamic influence matrices and describe the discretised dynamic response of the structure (displacements) to a unit impulse force and a unit plastic distortion applied in time step 0. All measurands being a linear combination of the displacements can be represented in a similar way. As an example, the corresponding strain evolution $\varepsilon_\alpha(t)$ can be represented using the so-called strain-displacement matrix $\boldsymbol{G}$, which relates displacements to strain field.

$$\varepsilon_\alpha(t) = \sum_{i=1}^{N} G_{\alpha i} u_i(t) = \sum_{\tau=0}^{t} \sum_{n \in \boldsymbol{L}} B^P_{\alpha n}(t-\tau)\, p_n(\tau) + \sum_{\tau=0}^{t} \sum_{\xi \in \boldsymbol{\Xi}} B^{\varepsilon}_{\alpha\xi}(t-\tau)\, \beta_{\xi}(\tau). \tag{2}$$

The dynamic influence matrices $\boldsymbol{B^P}$ and $\boldsymbol{B^{\varepsilon}}$ describe the strain evolution in time and can be either calculated or directly measured, e.g. with piezo transducers.

The elasto-plastic physical properties are described by a piecewise linear relation. The stress $\sigma_\alpha(t)$ in a plastified element $\alpha$ in time $t$ can be expressed in terms of the current value of the plastic distortion $\beta_\alpha(t)$ as well as in terms of the yield level $\sigma^* = E_\alpha \varepsilon^*$ and the hardening coefficient $\gamma_\alpha$

$$\sigma_\alpha(t) = E_\alpha \left[ \varepsilon_\alpha(t) - \beta_\alpha(t) \right], \qquad \sigma_\alpha(t) \mp \sigma^* = E_\alpha \gamma_\alpha \left[ \varepsilon_\alpha(t) \mp \varepsilon^*_\alpha \right], \tag{3}$$

where the sign depends on the stress sign. Combined together they yield

$$\beta_\alpha(t) = (1-\gamma_\alpha) \left[ \varepsilon_\alpha(t) \mp \varepsilon^*_\alpha \right], \tag{4}$$

where the strain $\varepsilon_\alpha(t)$ is expressed by Eq. (2). Eq. (4) rewritten for all plastified elements $\alpha$ can be transformed into a set of linear equations in unknowns $\beta_\alpha(t)$ and solved, time step by time step. Moreover, if the elements of the matrices $\boldsymbol{B}^P$ and $\boldsymbol{B}^\varepsilon$ vanish in time step 0, the distortion $\beta_\alpha(t)$ occurs only on the left hand side and thus can be directly computed in each time step, if the yield stress level is exceeded.

**Accelerations**

The nodal velocities can be expressed by direct differentiation of Eq. (1). In an obvious analogy to a continuous-time system

$$\begin{aligned}\dot{u}_i(t) = &\frac{1}{\Delta t}\sum_{n\in\boldsymbol{L}} D^P_{in}(0)\, p_n(t) + \frac{1}{\Delta t}\sum_{n\in\boldsymbol{L}} D^\varepsilon_{i\xi}(0)\,\beta_\xi(t) \\ &+\sum_{\tau=0}^{t}\sum_{n\in\boldsymbol{L}} \dot{D}^P_{in}(t-\tau)\, p_n(\tau) + \sum_{\tau=0}^{t}\sum_{\xi\in\boldsymbol{\Xi}} \dot{D}^\varepsilon_{i\xi}(t-\tau)\,\beta_\xi(\tau).\end{aligned} \tag{5}$$

A further differentiation would result in two troublesome components: the derivatives of the acting force $\partial p_n(t)/\partial t$ and of the plastic distortion $\partial\beta_\alpha(t)/\partial t$. A more convenient formula can be obtained by mixing the VDM formulation with the Newmark's integration scheme [8]. In each time step the displacements and the velocities can be calculated using the formulae Eq. (1) and Eq. (5), but the accelerations using the Newmark's constant integration parameters $a_0$, $a_2$ and $a_3$:

$$\ddot{u}_i(t) = a_0\big[u_i(t) - u_i(t-1)\big] - a_2\dot{u}_i(t-1) - a_3\,\ddot{u}_i(t-1)\,. \tag{6}$$

Therefore, if the discretised response is considered, the acceleration $\ddot{u}_n(t)$ is by Eq. (6), Eq. (5) and Eq. (1) a linear combination of acting forces $p_n(\tau)$ and plastic distortions $\beta_\alpha(\tau)$, the combination coefficients can be calculated iteratively and expressed in a way similar to Eq. (1):

$$\ddot{u}_i(t) = \sum_{\tau=0}^{t}\sum_{n\in\boldsymbol{L}} A^P_{in}(t-\tau)\, p_n(\tau) + \sum_{\tau=0}^{t}\sum_{\xi\in\boldsymbol{\Xi}} A^\varepsilon_{i\xi}(t-\tau)\,\beta_\xi(\tau). \tag{7}$$

## VDM: IMPACT FORCE RECONSTRUCTION

The identification task is formulated as an inverse problem and amounts to the minimisation of the objective function, which is a weighted sum of the mean-square distances between measured and modelled strains and accelerations.

**Objective function**

The identification aim is to determine the time evolution of the loading forces $p_n(t)$ that minimises the discrepancy between the measured and calculated structural behaviour. As both local strains and accelerations can be relatively easily measured, the objective function is composed of two weighted terms:

$$f(\boldsymbol{p}) = \frac{\sum_{t=0}^{T}\sum_{\alpha\in\boldsymbol{\Sigma}}\left[\varepsilon_\alpha^M(t)-\varepsilon_\alpha(t)\right]^2}{\sum_{t=0}^{T}\sum_{\alpha\in\boldsymbol{\Sigma}}\left[\varepsilon_\alpha^M(t)\right]^2} + \frac{\sum_{t=0}^{T}\sum_{i\in\boldsymbol{A}}\left[\ddot{u}_i^M(t)-\ddot{u}_i(t)\right]^2}{\sum_{t=0}^{T}\sum_{i\in\boldsymbol{A}}\left[\ddot{u}_i^M(t)\right]^2}. \tag{8}$$

Both terms represent scaled mean-square distances: the first between locally measured and calculated strains, while the second between locally measured and calculated accelerations. The weighting denominators are necessary to balance the influence of both components. The set of elements with strain gauges is denoted by $\boldsymbol{\Sigma}$, $\boldsymbol{A}$ denotes the the set of nodes with accelerometers.

**Gradients**

At the current stage of the research calculations of the gradient in the plastic case would involve a huge number of $O(T^3)$ components, where $T$ is the number of time steps. Therefore, this paper is limited to the case of elastic structures only.

The derivative of the objective function $f$ with respect to each unknown force $p_n(\tau)$ can be expressed in terms of the corresponding derivatives of $\varepsilon_\alpha(t)$ and $\ddot{u}_i(t)$:

$$\begin{aligned}\frac{\partial f(\boldsymbol{p})}{\partial p_n(\tau)} = &-2\left[\sum_{t=0}^{T}\sum_{\alpha\in\boldsymbol{\Sigma}}\left[\varepsilon_\alpha^M(t)\right]^2\right]^{-1}\sum_{t=0}^{T}\sum_{\alpha\in\boldsymbol{\Sigma}}\left[\varepsilon_\alpha^M(t)-\varepsilon_\alpha(t)\right]\frac{\partial\varepsilon_\alpha(t)}{\partial p_n(\tau)}\\ &-2\left[\sum_{t=0}^{T}\sum_{i\in\boldsymbol{A}}\left[\ddot{u}_i^M(t)\right]^2\right]^{-1}\sum_{t=0}^{T}\sum_{i\in\boldsymbol{A}}\left[\ddot{u}_i^M(t)-\ddot{u}_i(t)\right]\frac{\partial\ddot{u}_i(t)}{\partial p_n(\tau)},\end{aligned} \tag{9}$$

which in the elastic case ($\beta_\alpha(\tau)\equiv 0$) are easily calculated by Eq. (2) and Eq. (7)

$$\frac{\partial\varepsilon_\alpha(t)}{\partial p_n(\tau)} = B_{\alpha n}^P(t-\tau)\cdot\mathbf{1}_{\lfloor\tau\le t\rfloor}, \qquad \frac{\partial\ddot{u}_i(t)}{\partial p_n(\tau)} = A_{\alpha n}^P(t-\tau)\cdot\mathbf{1}_{\lfloor\tau\le t\rfloor}. \tag{10}$$

## EFFICIENT OPTIMISATION ALGORITHM

Force reconstruction is not straightforward due to the large number of unknowns $p_n(\tau)$ (number of time steps x number of optimised DOFs, 3,200 in the numerical example considered below). Nevertheless, a thorough analysis of the form of the objective function leads to an efficient optimisation procedure [9]. Further speed-up can be achieved by representing the space-time (i.e. $n$-$\tau$) distribution of acting forces $p_n(\tau)$ in the form of a linear combination of normalised atomic distributions:

$$p_n(\tau) = \sum_{m,\kappa} c_{m,\kappa}\cdot h_{m,\kappa}(n,\tau), \qquad \forall_{m,\kappa}\left[\sum_{n,\tau} h_{m,\kappa}(n,\tau)=1\right]. \tag{11}$$

The general accurate case is equivalent to the assumption $h_{m,\kappa}(n,\tau)=\mathbf{1}_{\lfloor n=m,\kappa=\tau\rfloor}$. The derivatives of the objective function $f$ with respect to the coefficients $c_{m,\kappa}$ can be easily calculated by Eq. (2), Eq. (7), Eq. (9) and the chain rule.

**Basic formulae**

The calculated strains Eq. (2) and accelerations Eq. (7) are linear combinations of the acting forces $p_n(\tau)$ and hence of the coefficients $c_{m,\kappa}$. Therefore, the objective function $f$ Eq. (8) is a convex *quadratic function* of $c_{m,\kappa}$ and can be exactly expanded around a given coefficient vector $\boldsymbol{c}=<c_{m,\kappa}>$

$$f(\boldsymbol{c}+\boldsymbol{d})=f(\boldsymbol{c})+\nabla f(\boldsymbol{c})^T\boldsymbol{d}+\frac{1}{2}\boldsymbol{d}^T\boldsymbol{H}\,\boldsymbol{d}\,, \tag{12}$$

where $\boldsymbol{H}$ is the (constant, positive semidefinite) Hessian of $f$ with respect to $c_{m,\kappa}$. The following formulae can be derived using Eq. (11), Eq. (12) and the linearity of calculated strains and accelerations (Eq. (2), Eq. (7)):

$$\begin{aligned}\nabla f(\boldsymbol{c})^T\boldsymbol{d}&=-2\,C_1\sum_{t=0}^{T}\sum_{\alpha\in\boldsymbol{\Sigma}}\varepsilon_\alpha^{(\boldsymbol{d})}(t)\left[\varepsilon_\alpha^{M}(t)-\varepsilon_\alpha^{(\boldsymbol{c})}(t)\right]-2\,C_2\sum_{t=0}^{T}\sum_{i\in\boldsymbol{A}}\ddot{u}_i^{(\boldsymbol{d})}(t)\left[\ddot{u}_i^{M}(t)-\ddot{u}_i^{(\boldsymbol{c})}(t)\right],\\ \boldsymbol{d}_i^T\boldsymbol{H}\,\boldsymbol{d}_j&=2\,C_1\sum_{t=0}^{T}\sum_{\alpha\in\boldsymbol{\Sigma}}\varepsilon_\alpha^{(\boldsymbol{d}_i)}(t)\cdot\varepsilon_\alpha^{(\boldsymbol{d}_j)}(t)+2\,C_2\sum_{t=0}^{T}\sum_{i\in\boldsymbol{A}}\ddot{u}_i^{(\boldsymbol{d}_i)}(t)\cdot\ddot{u}_i^{(\boldsymbol{d}_j)}(t)\,,\end{aligned} \tag{13}$$

where $C_1$ and $C_2$ denote the weighting coefficients (inverse of the denominators in Eq. (8)); $\varepsilon_\alpha^{(\boldsymbol{c})}(t)$, $\ddot{u}_i^{(\boldsymbol{c})}(t)$ denote the strains and accelerations calculated with Eq. (2) and Eq. (7) for the loading defined by the coefficient vector $\boldsymbol{c}=<c_{m,\kappa}>$ and Eq. (11).

**Line optimisation**

Even for simple structures the Hessian occurring in Eq. (12) is too large to compute and invert it directly, which would be necessary to find the minimum in one step only. Therefore, a series of line optimisations has to be performed; each step amounts to finding at a given point $\boldsymbol{c}$ the line minimum along a direction $\boldsymbol{d}$, i.e. the value of $s$ that minimises $f(\boldsymbol{c}+s\cdot\boldsymbol{d})$, which is a convex quadratic function. The summands in Eq. (12) can be directly calculated using the formulae Eq. (13). Thus

$$s_{min}=-\frac{\nabla f(\boldsymbol{c})^T\boldsymbol{d}}{\boldsymbol{d}^T\boldsymbol{H}\,\boldsymbol{d}}. \tag{14}$$

**Conjugate directions**

The steepest descent method assumes $\boldsymbol{d}=-\nabla f(\boldsymbol{c})$ at each optimisation step, but it suffers from slow convergence. However, the objective function $f$ is an unbounded quadratic form, hence choosing in each step a direction $\boldsymbol{d}_{n+1}$ *conjugate* with all previous directions $\boldsymbol{d}_0$, ..., $\boldsymbol{d}_n$ leads by Eq. (14) directly to the minimum in the whole subspace generated by all considered directions. Therefore, starting with the steepest descent direction and making use of the conjugacy criterion $\boldsymbol{d}_i^T\boldsymbol{H}\boldsymbol{d}_j=0$,

$$\boldsymbol{d}_{n+1}=-\nabla f(\boldsymbol{c}_{n+1})+\sum_{i=0}^{n}\eta_i\boldsymbol{d}_i,\quad\text{where}\quad\eta_i=\frac{\nabla f(\boldsymbol{c}_{n+1})^T\boldsymbol{H}\,\boldsymbol{d}_i}{\boldsymbol{d}_i^T\boldsymbol{H}\,\boldsymbol{d}_i}. \tag{15}$$

## The algorithm

The most expensive in the algorithm below are the calculations of the gradient and of the corresponding initial response. Moreover, at large step numbers $n$, it is faster to calculate the final response directly than to superpose the stored responses.

Initial calculations:

initialise: $\boldsymbol{c}_0=\boldsymbol{0}$ and $\varepsilon_\alpha^{(\boldsymbol{c}_0)}(t)=\boldsymbol{0}$, $\ddot{u}_i^{(\boldsymbol{c}_0)}(t)=\boldsymbol{0}$

calculate $\boldsymbol{d}_0=-\nabla f(\boldsymbol{p}_0)$ and $\varepsilon_\alpha^{(\boldsymbol{d}_0)}(t)$, $\ddot{u}_i^{(\boldsymbol{d}_0)}(t)$

normalise: $D=\sqrt{\boldsymbol{d}_0^T\boldsymbol{H}\,\boldsymbol{d}_0}$ and $\boldsymbol{d}_0=\boldsymbol{d}_0/D$, $\varepsilon_\alpha^{(\boldsymbol{d}_0)}(t)=\varepsilon_\alpha^{(\boldsymbol{d}_0)}(t)/D$, $\ddot{u}_i^{(\boldsymbol{d}_0)}(t)=\ddot{u}_i^{(\boldsymbol{d}_0)}(t)/D$

calculate the line minimum $s=-\nabla f(\boldsymbol{c}_0)^T\boldsymbol{d}_0$

store $\boldsymbol{d}_0$ and $\varepsilon_\alpha^{(\boldsymbol{d}_0)}(t)$, $\ddot{u}_i^{(\boldsymbol{d}_0)}(t)$

The loop:

update: $\boldsymbol{c}_{n+1}=\boldsymbol{c}_n+s\cdot\boldsymbol{d}_n$ and $\varepsilon_\alpha^{(\boldsymbol{c}_{n+1})}(t)=\varepsilon_\alpha^{(\boldsymbol{c}_n)}(t)+s\cdot\varepsilon_\alpha^{(\boldsymbol{d}_n)}(t)$, $\ddot{u}_i^{(\boldsymbol{c}_{n+1})}(t)=\ddot{u}_i^{(\boldsymbol{c}_n)}(t)+s\cdot\ddot{u}_i^{(\boldsymbol{d}_n)}(t)$

calculate $\boldsymbol{d}_{n+1}=-\nabla f(\boldsymbol{c}_{n+1})$ and $\varepsilon_\alpha^{(\boldsymbol{d}_{n+1})}(t)$, $\ddot{u}_i^{(\boldsymbol{d}_{n+1})}(t)$

conjugate direction: for (i = 0; i <= n; ++i)

$\eta=-\boldsymbol{d}_{n+1}^T\boldsymbol{H}\,\boldsymbol{d}_i$

$\boldsymbol{d}_{n+1}=\boldsymbol{d}_{n+1}+\eta\cdot\boldsymbol{d}_i$ and $\varepsilon_\alpha^{(\boldsymbol{d}_{n+1})}(t)=\varepsilon_\alpha^{(\boldsymbol{d}_{n+1})}(t)+\eta\cdot\varepsilon_\alpha^{(\boldsymbol{d}_i)}(t)$, $\ddot{u}_i^{(\boldsymbol{d}_{n+1})}(t)=\ddot{u}_i^{(\boldsymbol{d}_{n+1})}(t)+\eta\cdot\ddot{u}_i^{(\boldsymbol{d}_i)}(t)$

normalise:

$D=\sqrt{\boldsymbol{d}_{n+1}^T\boldsymbol{H}\,\boldsymbol{d}_{n+1}}$ and $\boldsymbol{d}_{n+1}=\boldsymbol{d}_{n+1}/D$, $\varepsilon_\alpha^{(\boldsymbol{d}_{n+1})}(t)=\varepsilon_\alpha^{(\boldsymbol{d}_{n+1})}(t)/D$, $\ddot{u}_i^{(\boldsymbol{d}_{n+1})}(t)=\ddot{u}_i^{(\boldsymbol{d}_{n+1})}(t)/D$

calculate the line minimum $s=-\nabla f(\boldsymbol{c}_{n+1})^T\boldsymbol{d}_{n+1}$

store $\boldsymbol{d}_{n+1}$ and $\varepsilon_\alpha^{(\boldsymbol{d}_{n+1})}(t)$, $\ddot{u}_i^{(\boldsymbol{d}_{n+1})}(t)$

## NUMBER OF SENSORS AND FURTHER SPEED-UP

Several ideas to speed-up the optimisation process and reduce the number of sensors can be considered. They can be either purely numeric or can rely on heuristics derived from engineering common sense and/or post-accident on-site inspection (number and size of impact areas, possible impact locations etc.).

The time complexity of each algorithm step is $O(CST^2)$, where $C$ is the number of distributions being superposed (coefficients $c_{m,\kappa}$), $S$ is the number of sensors and $T$ is the number of time steps. An obvious idea is to divide a long time interval into several (not too short) subintervals and to perform the optimisation for each of them separately, assuming the loading identified in the preceding subintervals is accurate. Another idea can utilise the fact that impact is a short and localised event, hence most of the acting forces and the coefficients $c_{m,\kappa}$ are zero. Thus, to reduce the number of unknowns $C$ the identification can be split into phases: initial phases use a limited number of fuzzy atomic distributions (possibly including space search) to identify impact areas, followed by phases of localised, more accurate identification.

Minimisation of the objective function $f$ corresponds to solving a large-scale linear system. To guarantee the uniqueness of the solution the unknowns shall not exceed in number the equations, provided the system is not singular. Hence, the number of distributions being superposed $C$ shall not exceed the total number of measurements $\varepsilon_\alpha^M(t)$ and $\ddot{u}_n^M(t)$ (time steps x the number of sensors). Otherwise there would exist a subspace of feasible solutions, which would result in the same structural response in sensor locations. Measurement noise, inevitable in a real system, may increase the required number of sensors.

Thus a restriction of the search in space and/or time can reduce both the number of necessary sensors and the optimisation time. Moreover, the objective function can be modified to include a measure of variation of identified force evolutions as in [4]; this would significantly reduce the number of necessary sensors but make the process heavily relying on the heuristic assumption of force smoothness: it would identify *the smoothest*, but not necessarily *the actual* loading.

## NUMERICAL EXAMPLE

Fig. 1 shows the modelled elastic truss structure. It is 4 m x 2 m; the elements are 66 mm$^2$ in cross-section, 0.5 m or $0.5\sqrt{2}$ m long, and made of steel (7,800 kg/m$^3$; 200 GPa). Strain sensors were located in the 32 diagonal elements of the bottom plane. The left hand side corner nodes were deprived of all degrees of freedom, while the right hand side corner nodes were free in horizontal directions only.

### Simulated impact forces

The simulated loading modelled a vertical force moving along the numbered nodes across the structure (Fig. 1), thus it was triangular in shape in each node, see Fig. 2. The corresponding strains in sensor locations have been calculated and stored to model the measurements $\varepsilon_\alpha^M(t)$.

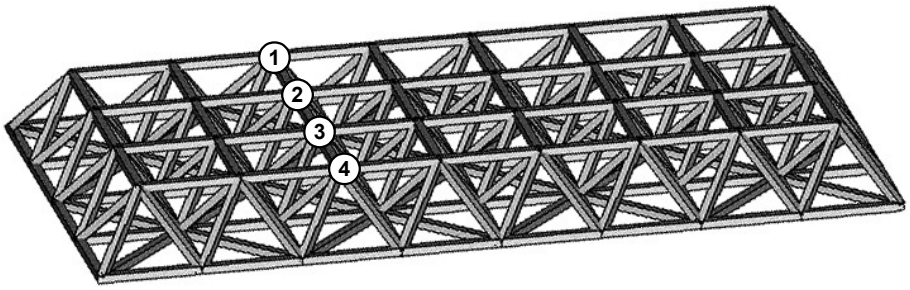


FIGURE 1 Elastic truss structure modelled in the numerical example

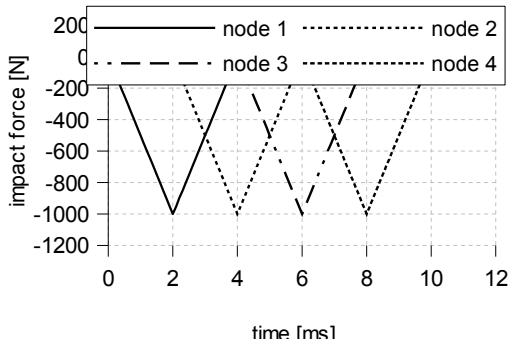


FIGURE 2 Simulated loading model
a vertical force moving along the nodes 1, 2, 3, 4

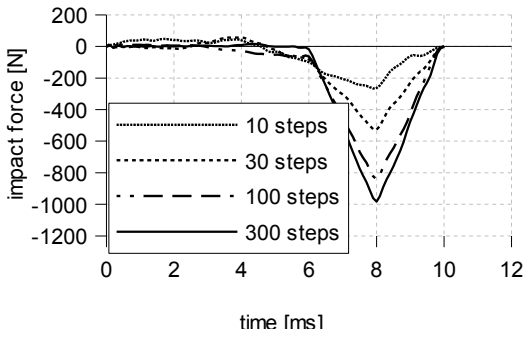


FIGURE 3 Impact forces identified in node 4
(respective optimisation time: 3 s, 10 s, 33 s, 108 s)

### Impact identification

An accurate identification has been performed: $h_{m,\kappa}(n,\tau)=\mathbf{1}_{(n=m,\kappa=\tau)}$. There are 32 strain sensors, hence force evolutions in all 32 vertical DOFs of the top plane can be simultaneously identified. The time interval of 10 ms was divided into 100 time steps, 300 optimisation steps were made. Fig. 3 shows as an example the identified vertical force evolution in node 4 after 10, 30, 100 and 300 optimisation steps, the respective optimisation times on a desktop PC were 3 s, 10 s, 33 s and 108 s.

## CONCLUSIONS AND FURTHER WORK

A robust methodology for impact load identification is described. It includes simultaneous multiple impact and moving load cases and is based on local strain and/or acceleration measurements, which can be stored in a black box system for reliable a posteriori reconstruction of accident scenario.

The research is ongoing to reduce the number of necessary sensors and verify the described heuristics, investigate the issues of the best sensor locations and the sensitivity to measurement noise. A corresponding algorithm for plate structures is currently being tested and an experimental verification is prepared.

## ACKNOWLEDGEMENT

The authors gratefully acknowledge the financial support through the Polish Research Project MAT-INT (PBZ-KBN-115/T08/2004) and the 5FP EU Research Training Network SMART SYSTEMS (HPRN-CT-2002-00284). This paper is the final degree work done by the first author at the course of Smart Technology Expert School, operating at the Institute of Fundamental Technological Research, Poland.

## REFERENCES

1. T. M. Kowalick, *Fatal Exit: The Automotive Black Box Debate*, Wiley-IEEE Press, Nov. 2004.
2. H. Gabler, D. Gabauer, H. Newell, M. O'Neill, NCHRP Web-Only Document #75: *Use of Event Data Recorder (EDR) Technology for Highway Crash Data Analysis*, Dec. 2004.
3. J. Holnicki-Szulc, J. T. Gierlinski, *Structural Analysis, Design and Control by the Virtual Distortion Method*, John Wiley & Sons, Chichester, U.K., 1995.
4. H. Fukunaga, N. Hu, *Health monitoring of composite structures based on impact force identification*, Proc. of the 2nd European Workshop on SHM, Munich, 2004, pp. 415-422.
5. S. M. Peelamedu, C. Ciocanel, N. G. Naganathan, *Impact detection for smart automotive damage mitigation systems*, Smart Mater. Struct., Vol. 13, 2004, pp. 990-997.
6. R. Seydel, F.-K. Chang, *Impact identification of stiffened composite panels: I. System development*, Smart Mater. Struct., Vol. 10, 2001, pp. 354-369.
7. J. Holnicki-Szulc, P. Pawlowski, M. Wiklo, *High-performance impact absorbing materials - the concept, design tools and applications*, Smart Mater. Struct., Vol. 12, No. 3, 2003.
8. K. Bathe, *Finite Element Procedures*, Prentice-Hall, Englewood Cliffs, New Jersey 1996.
9. M. Wiklo, L. Jankowski, J. Holnicki-Szulc, *Impact load identification - forensic engineering*, to appear in: Proc. of the 2nd Int. Conf. on Nonsmooth Nonconvex Mechanics, NNMAE 2006, Thessaloniki, Greece,